Combining Spectral and Active Shape Methods to Track Tagged MRI

Jaume GARCIA-BARNÉS [+], Petia RADEVA [+], Francesc CARRERAS [*]
[+] *Centre de Visió per Computador – Dept. Informàtica, UAB, Barcelona, Spain*
[*] *Hospital de la Santa Creu i de Sant Pau, Barcelona, Spain*
{jaumegb,petia}@cvc.uab.es

Abstract. Tagged magnetic resonance is a very usefull and unique tool that provides a complete local and global knowledge of the left ventricle (LV) motion. In this article we introduce a method capable of tracking and segmenting the LV. Spectral methods are applied in order to obtain the so called HARP images which encode information about movement and are the base for LV point-tracking. For segmentation we use Active Shapes (ASM) that model LV shape variation in order to overcome possible local misplacements of the boundary. We finally show experiments on both synthetic and real data which appear to be very promising.

Keywords. MR, tagged MR, ASM, LV segmentation, motion estimation.

1. Introduction

Heart diseases are one of the most common death causes of the last decades. For this reason, it is important to develop tools that allow clinicians to obtain quantitative data to provide a good diagnosis and derive an appropriate treatment that can turn to a significant reduction of mortality. *Magnetic Resonance* (MR) is the most common, non-invasive, cardiac imaging technique as it can provide, into a single sequence examination, information about anatomy, structure, global and regional function and contraction of the heart. Nevertheless, the lack of identifiable landmarks within the myocardium (Figure 1.a) makes motion assessment limited due to the fact that many patients may have significant regional dysfunction while maintaining an ejection fraction relatively within normal limits.

To overcome this limitation, a new image modality is designed: *Tagged Magnetic Resonance* (TMR) (Figure 1.b), which uses a special pulse sequence to spatially modulate the longitudinal magnetization of the subject prior to acquiring image data. This is called spatial modulation of magnetization (SPAMM) and produces a grid over the myocardium, which deforms by the underlying motion of the heart. Thus, inner tissue deformation becomes visible, allowing for other pathologies to be assessed.

Despite the potential of this imaging technique, it has not become a clinical standard in part because of the difficulty for the clinicians to manage and quantify all the information as well as because any post processing of the images is extremely time consuming. Regard that each analysis assumes manually tracking about 100 points per frame, 10 frames per sequence and 10 sequences belonging to different heart slices per scan session (aprox.). This justifies the need for specific software that can extract quantitative data in a relatively short time. Numerous analyses to detect tag features have been developed and all of them need of the application of some interpolation process in order to get dense motion

estimations, i.e., at every point. Guttman *et al.*[1] used morphological image processing and matched filtering techniques [1], Young and Axel [2] and Kumar and Goldgof [3] use deformable meshes. Young an Axel have used manually identified points [2]. To interpolate dense motion Young and Axel [2] used a finite element model, O'Dell *et al.*[4] used truncated polynomial expansion, Denney and Prince [5] used stochastic estimation scheme, Radeva *et al.*[6] used 3D B-splines and Ozturk and McVeigh [13] used 4D B-splines.

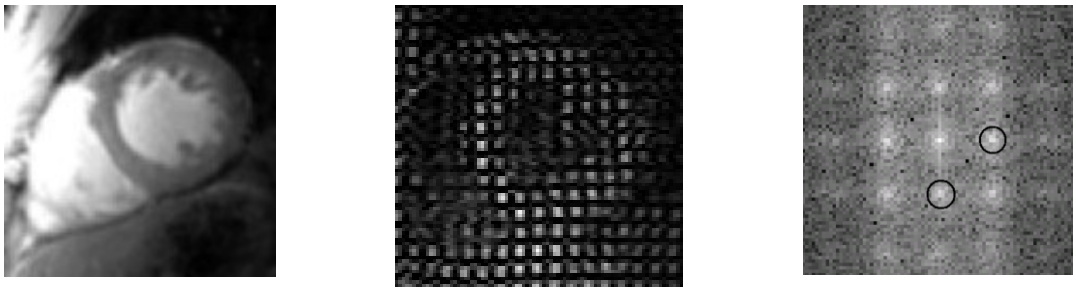

(a) (b) (c)

Figure 1 (a) Ordinary MR. We can appreciate the lack of identificlable points into the myocardium. (b) TMR. Dark stripes gives us a way to observe the evolution of inner points in the myocardium. (c) TMR Fourier transform with the main harmonic peaks in orthogonal directions to be filtered.

The method we use in this paper for cardiac tagged MR analysis was developed by Osman *et al.*[7] and it is based on the so called HARP (harmonic phase) images. It provides us a method to get dense motion estimation, i.e., we can estimate the trajectory of any point in the myocardium, and thus no interpolation process must be done.

What is new in this work is to exploit the information provided by the previous method to segment the myocardium. Given an initial segmentation of the first frame, it will evolve for each frame according to the displacement map provided by the method. The drawback is that the lack of tags outside the myocardium affects the displacement estimation at the myocardium borders (epicardium and endocardium) and this may cause the segmentation evolution fail. For this reason in this work we propose to incorporate a priori knowledge; more precisely, we propose to use *active shape models* (ASM) to create a model of the left ventricle myocardium to ensure that local errors are corrected by the global influence of the shape. We describe a complete method, based on HARP images and ASM, that allows to fully analyse the myocardial function and which is the base for further extraction of any kind of quantitative data such as stress or strain parameters. One more consideration about the segmentation is that if we combine, at each step with the motion estimation process, we can avoid calculus on outer LV points that are not desired.

The article is organized as follows: in section 2 we explain the fundamentals of the tagging process and HARP images. In section 3 we show how HARP images can be used to track small motions of the myocardium. In section 4 we expose our segmentation algorithm and provide a short overview of ASM theory. In section 5 we show experimental results on both synthetic and real data and finally, in section 6 we extract conclusions of this work.

2. HARP images

The key point in tagged MR image is not to study them in the spatial domain but in the frequency domain. We appreciate in figure 1.c a collection of spectral peaks, which contain

information about motion, each of them in a certain direction. If we filter one of these peaks, back in the spatial domain we get a complex image the phase of which is linearly related to the directional component of the true motion. Obtaining the phase is quite difficult, even though we will see that the principal values of the phase, lying in [-π , π], are enough to estimate small motions.

2.1 SPAMM tagging

The tagging process consists of applying to the transverse magnetization, present in the ordinary MR images, one or more gradient pulses that produce a periodic spatial modulation of the phase. The pulse is applied at end diastole $(t = 0)$, when the left ventricle is full of blood and the heart is relatively slowly moving.

The tag pattern can be considered as a function $f(p;g_1,g_2)$ [8] with $|f(p;g_1,g_2)| \le 1$, that modulates the underlying magnetisation intensity of every material point p at time $t = 0$:

$$f(p;g_1,g_2) = \sum_{n=0}^{N-1} a_n \cos(n g_1^T p) \sum_{n=0}^{N-1} a_n \cos(n g_2^T p)$$

where N are the number of pulses and g_1 and g_2 are orthogonal gradient directions. For more details about a_n coefficients, see [8]. So at time $t = 0$, the resultant image is given by $I(p;g_1,g_2) = I_0(p)\, f(p;g_1,g_2)$, where $I_0(p)$ is the image at end-diastole without tags. Managing equations one get the following

$$I(p;w_k) = \sum_{k=1}^{K} I_0(p) c_k e^{i w_k^T p} = \sum_{k=1}^{K} I_k(p;w_k)$$

with $K = (2N-1)^2$. This is the formulation of the first frame. The reference frame, where its points are considered to be material points expected to be moved. As the heart deforms, a material point within the myocardium moves from its reference position p to a new spatial position x at time t and it is given by the reference map $p(x,t)$ so, for any frame in the sequence, we have the formulation

$$I(x,t) = \sum_{k=1}^{K} I_0(p(x,t)) c_k e^{i w_k^T p(x,t)} = \sum_{k=1}^{K} I_k(x,t)$$

It is worth to say that despite the true motion of the heart is in 3D, in this work we consider just the apparent motion that is in 2D. This means that we assume that the gradient directions of the tagging pulse are parallel to the image plane thus, what we see in the images are projections of the real movement. Some works as [14] track the 3D cardiac motion using perpendicular views of the myocardium, short axis and long axis.

2.2 Frequency domain analysis

Due to the fact that the cosine function has two symmetric spectral peaks in the Fourier domain, we get exactly $(2N-1)^2$ spectral peaks which locations are easy to find from

g_1 and g_2. Each of these peaks corresponds, approximately, to the Fourier transform of $I_k(x,t)$ because most of its energy around it thus, by filtering it [9] one can separate $I_k(x,t)$ from $I(x,t)$. I_k is called the *k*th harmonic image. Notice that $I_k \in \mathbf{C}$ and for this reason, we can get both the real and the imaginary part. What is interesting for us is precisely the last one. The phase is given by $\varphi_k(x,t) = w_k^T p(x,t)$ what shows that the frequency is linearly related to the phase. We will not be able to calculate the phase due to the *arc tang* operator wrapping effect but instead we define the HARP image (Figure 2) as following

$$a_k(x,t) = \angle I_k(x,t) = \begin{cases} \tan^{-1}\left(\dfrac{\mathrm{Im}\{I_k\}}{\mathrm{Re}\{I_k\}}\right), & \mathrm{Re}\{I_k\} \geq 0 \\ \tan^{-1}\left(\dfrac{\mathrm{Im}\{I_k\}}{\mathrm{Re}\{I_k\}}\right) + \pi, & \text{otherwise} \end{cases}$$

(a) (b)

Figure 2 HARP images obtained by filtering two of the principal harmonics in orthogonal direction, vertical (a) and horizontal (b).

3. Motion tracking using HARP images

In this section we describe how to estimate apparent motion for small displacements using HARP images. To any point in the image we can associate a pair of angles, one for each HARP image. We define this pair as $\varphi = [\varphi_h \ \varphi_v]^T$ where φ_h is the horizontal component and φ_v the vertical one. Now, given a point in the *m*th frame x_m we would like to find x in the *(m+1)*th frame that fulfils the condition $\varphi(x, t_{m+1}) = \varphi(x_m, t_m)$ or equivalently, to find a solution to the multidimensional non-linear, root finding problem $\varphi(x, t_{m+1}) - \varphi(x_m, t_m) = 0$ which can be solved by applying the Newton-Raphson iteration method $x^{(n+1)} = x^{(n)} - \left[\nabla\varphi(x^{(n)}, t_{m+1})\right]^{-1}\left[\varphi(x^{(n)}, t_{m+1}) - \varphi(x_m, t_m)\right]$. For details about the practical implementation see [10]. We define the *displacement map* as $u(x,t) = \hat{x} - x$ where $\hat{x}$ satisfies the previous non-linear equation: $\varphi(\hat{x}, t+1) - \varphi(x,t) = 0$.

This method gives dense motion estimation for any point in the image. Nevertheless we want only to track points in the myocardium. For this reason, if we have the LV segmented, we can avoid make useless calculations over non-desired points, apart from the intrinsic importance of having our object of interest localized.

4. LV Segmentation

As we discussed before, the aim of this work is to give a complete framework for LV analysis in two aspects: tracking of any point in the myocardium and segmenting it. The segmentation we propose is based on the displacement map given by the HARP motion estimation and it allows to avoid calculations over points out of the myocardium which are not of interest. The process follows these steps: we segment the first frame, which can be done manually (minimal human interaction). Once we have the initial segmentation, we can calculate the displacement map (just over the points in the region of interest). Due to the fact that we have the estimation where any point will move in the next frame, in particular, we can estimate next segmentation. Nevertheless due to the lack of tags out of the myocardium, it can make the segmentation locally fail. It is for this reason that we apply Active Shape Models, which allow correcting possible local misplacements of the estimated boundary as it is a global method that seeks for a valid shape that fits best all the points.

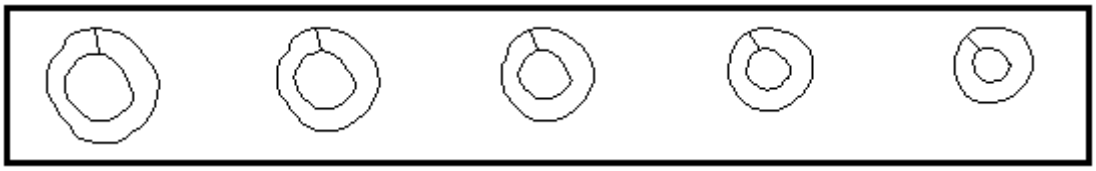

Figure 3 First variation mode of our LV linear model. The central shape is the mean shape and the other shapes are obtained by varying the first component of parameter *b*.

4.1 Active Shape Models

This technique allows to build compact models of shape by capturing the statistics of sets of labelled points in a set of training images. Once the model is built, only plausible shapes (similar to the ones in the training set) can be obtained [11]. Having *N* training images, manual segmentation is performed on every image I_j. Let $\tilde{s}_j = \{(\tilde{x}_j, \tilde{y}_j)\}_{i=1}^{M}$ be the ordered set of its landmark coordinates. We align $\tilde{s}_j$ to a reference shape s_0 by applying a transformation $s_j = L_{r,\theta,T}(\tilde{s}_j)$ that scales, rotates and translates s_j. This process is done using Procrustes analysis and allows to capture the intrinsic variation of shapes avoiding similarities. Let $\{(x_j, y_j)\}_{i=1}^{M}$ be the aligned coordinates of the *j*th training image, we construct the vector $X_j = (x_1^j, y_1^j, x_2^j, y_2^j, \cdots, x_N^j, y_N^j)$ by concatenating the coordinates of the points. Applying *Principal Component Analysis* (PCA) to the data, we reduce the dimensionality while maintaining relevant information. Any shape in the training shape can now be approximated using the mean shape $\overline{X} = 1/N \sum_{j=1}^{N} X_j$ and a linear combination of the first $m < M$ modes of variation $X = \overline{X} + Pb$ where $P = (P_1, P_2, \ldots, P_m)$ is the matrix of the first *m* modes with $P^T P = Id$ and $b = (b_1, b_2, \ldots, b_m)$ is the shape parameter vector. If we have an aligned shape $\tilde{X}$, and we want to find the most similar plausible shape, we just have to project it into the space to get the parameter vector b, $b = P^T(\tilde{X} - \overline{X})$ and ensure

that b lives into a certain valid *m*-dimensional hyper box. Then plausible shape is exactly $X = \overline{X} + Pb$.

3.2 Segmentation algorithm

Given an initial segmentation of the first frame characterised by a set of points $S^0 = \{X_i^0\}_{i=1}^N$ and the segmentation in the *j*th step $S^j = \{X_i^j\}_{i=1}^N$, we estimate the next segmentation result using the displacement map as follows: $\tilde{S}^{j+1} = \{X_i^j + u(X_i^j, j)\}_{i=1}^N = \{\tilde{X}_i^j\}_{i=1}^N$. Then to overcome possible local misplacements we seek for a valid shape in our Shape Model that best fits the estimated points: for every *i* we obtain the parameter in the shape space b_{j+1} as we discussed in the previous section and get the valid shape as $S^{j+1} = \overline{X} + Pb_{j+1}$

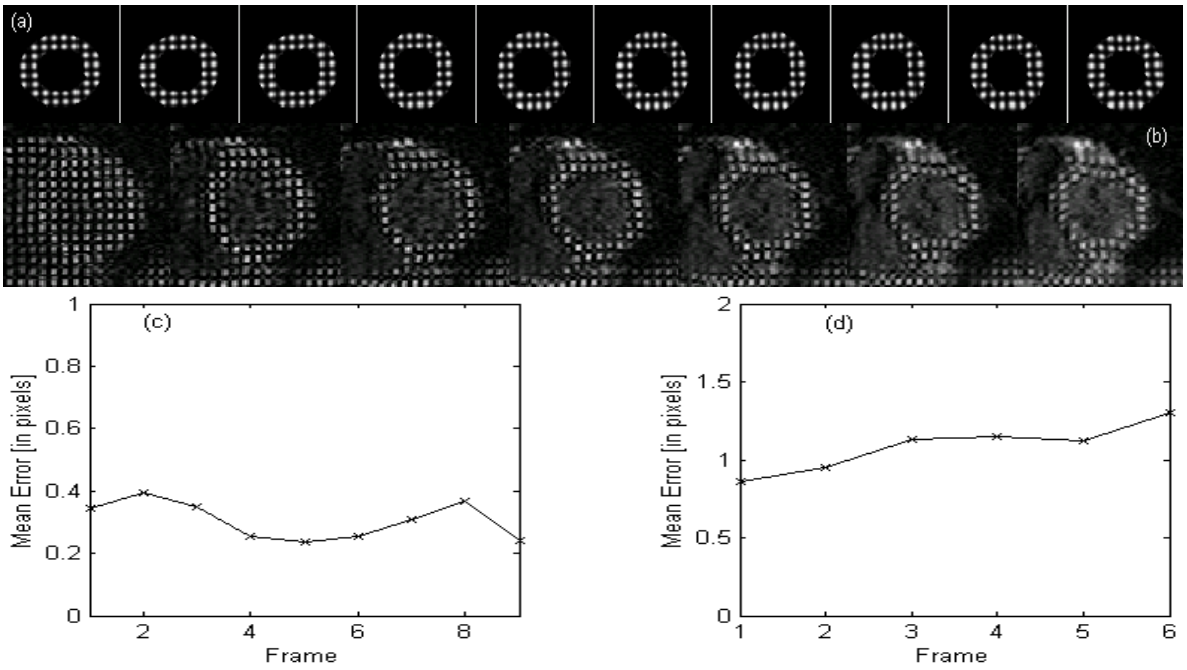

Figure 4 (a) Synthetic tagged MR sequences. (b) Real tagged MR sequences. (c) & (d) Mean of the distance errors obtained for every synthetic and real sequences, respectively.

5. Experimental results

In this section we show the performance of the two algorithms: motion estimation and LV segmentation using both synthetic and real data.

We have created a 2D synthetic model (Figure 4.a) based on the work presented in [12], that allows to create tagged MR sequences and which is governed by six parameters (translation in x and y, rotation, shear, eliptication and radial compression). From the synthetic sequence we know exactly its displacement map, which will be compared to the one given by the algorithm. Five synthetic sequences have been created and for each of them we have calculated the difference between both displacement maps at every point. Mean difference have been extracted (Figure 4.c). Notice that error is less than 0.4 pixels. To test the algorithm on real data, we have used 5 sequences similar than in figure 4.b and

for them we have manually marked points to obtain a discrete displacement map over which we have compared the displacement map provided by the algorithm. Also mean distance has been calculated for these points and shown in figure 4.d. The mean error is about 1 pixels and it increases as the sequence evolve due to the fact that tagged MR sequences loses tag contrast in time.

To test the segmentation algorithm we used the same real data and to create the linear model of the LV shape, we used a training set of 50 images manually segmented using 32 landmarks for this purpose. After applying the PCA to the points, we have obtained an 8-dimensional linear model that explain the 98.75% of shape variation. In figure 3 we can appreciate the first main mode of variation. We empirically show the performance of our segmentation algorithm in figure 5.a and 5.b. Due to the fact that the base of the segmentation is the displacement map, error in segmentation is, as much as the one given by HARP method but, in addition, ASM often reduces it due to its a priori shape knowledge incorporation. In figure 5.c .d and .e we show the displacement map restricted to the LV (region of interest).

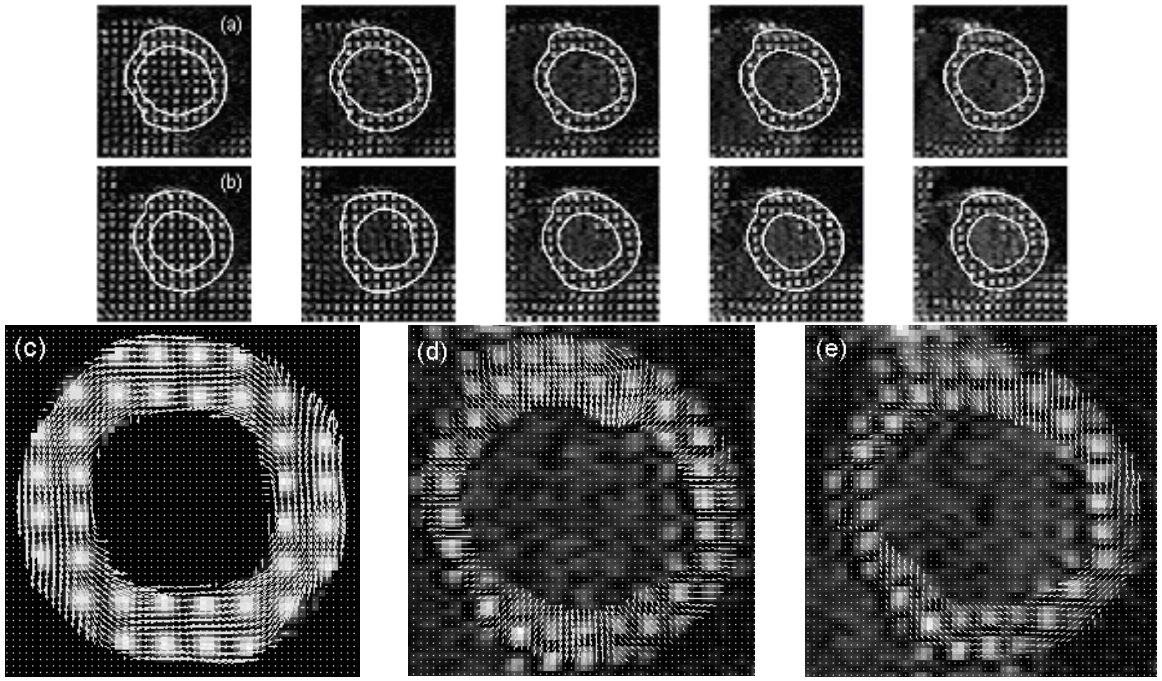

Figure 5 (a) and (b) output of our segmentation algorithm. (c), (d) and (e) detail of the dense displacement map for a synthetic and a real tagged images.

6. Conclusions

In this article we overview an interesting method that exploits the frequential nature of tagged MRI and which does not need further interpolation processes to obtain dense motion estimations. Taking advantage of this information we developed a segmentation method that is supervised by a shape model that acts as a correction factor. Thus, given a tagged MRI sequence, we described the framework to localize the object of interest, the LV (segmentation) and track its points. This gives the base for any kind of quantitative data extraction for further interpretation or simulation.

References

[1] M.A. Guttman, J.L. Prince, and E.R. McVeigh, “Tag and contour detection in tagged MR images of the left ventricle”, IEEE Trans. Med. Imag., vol. 13, pp. 74–88, 1994.

[2] A.A. Young and L. Axel, “Three-dimensional motion and deformation of the heart wall: Estimation with spatial modulation of magnetization— A model based approach”, Radiology, vol. 185, pp. 241–247, 1992.

[3] S. Kumarand D. Goldgof, “Automatic tracking of SPAMM grid and the estimation of deformation parameters from cardiac MR images”, IEEE Trans. Med. Imag., Mar. 1993.

[4] W.G. O'Dell, C.C. Moore, W.C. Hunter, E.A. Zerhouni, and E.R. McVeigh, “Three-dimensional myocardial deformations: Calculations with displacement field fitting of tagged MR images”, Radiology, vol. 195, pp. 829–835, 1995.

[5] T.S. Denney and J.L. Prince, “Reconstruction of 3-D left ventricular motion from planar tagged cardiac MR images: An estimation theoretic approach”, IEEE Trans. Med. Imag., vol. 14, pp. 625–635, 1995.

[6] P. Radeva, A. Amini,J. Huang, and E. Marti, “Deformable B-solids and implicit snakes for localization and tracking of SPAMM MRI-data”, in Proc of MMBIA, 1996, pp. 192–201.

[7] N.F. Osman, E.R. McVeigh, and J.L. Prince, “Imaging Heart Motion Using Harmonic Phase MRI”, in IEEE Trans. Med. Imag., vol.19, pp. 186-202, 2000.

[8] W.S. Kerwin, N.F. Osman, and J.L. Prince, “Image processing analysis in tagged cardiac MRI”, Chapter 24, Handbook of Medical Image Processing, I Bankman , Academic Press, 2000.

[9] N.F. Osman, and J.L. Prince, “On the design of bandpass filters in harmonic phase MRI”, IEEE Image Processing Proceedings, vol.1, pp. 625 – 628, 2000.

[10] N.F. Osman, W.S. Kerwin, E.R. McVeigh, and J.L Prince, “Cardiac motion tracking using CINE harmonic phase (HARP) magnetic resonance imaging”, Megnetic Resonance in Medicine 42, pp. 1048-1060, 1999.

[11] T. Cootes, C. Taylor, D. Cooper, and J. Graham, “Active Shape Models - Their Training and application”, Computer Vision and Image Understanding 1995; 61(1):38-59.

[12] E. Waks, J.L. Prince, and A. Douglas, ”Cardiac Motion Simulator for Tagged MRI”, Proceedings of the IEEE Workshop on Mathematical Methods in Biomedical Image Analysis, San Francisco June 21--22, 1996.

[13] C. Ozturk and E. McVeigh, “Four dimensional B-spline based motion analysis of tagged cardiac MR images, SPIE Medical Imaging, San Diego, CA, February 1999.

[14] L. Pan, J.A.C. Lima and N.F. Osman, “Fast tracking of cardiac motion using 3D-HARP”.